Effect of non-local near-resonant interactions of Rossby waves on formation of large-scale zonal flows in unforced two-dimensional turbulence on rotating sphere

Yusuke Hagimori[1], Kiori Obuse[1,*], and Michio Yamada[2]
1: *Graduate School of Environmental, Life, Natural Science* and Technology, Okayama university,
Okayama 700-8530, Japan
2 *Research Institute for Mathematical Sciences, Kyoto University, Kyoto 606-8502, Japan*

February 23, 2024

Abstract

This study investigates the effect of nonlinear interactions of Rossby waves on large-scale zonal flow formation in two-dimensional turbulence on a rotating sphere. The coefficients of nonlinear interactions are first calculated. Then, the non-local, near-resonant, and non-local near-resonant interactions are investigated in detail. The results show that the formation of large-scale westward circumpolar zonal flows is directly caused by non-local energy transfer due to the three-wave near-resonant interactions of Rossby waves.

1 Introduction

Fluid dynamics in rotating systems has attracted much attention in recent years due to advances in computing technology and growing environmental

*obuse@okayama-u.ac.jp

concern. The rotation effect of the system brings about some outstanding phenomena, such as the spontaneous formation of large-scale zonal flows, which has been numerically confirmed even for one of the simplest systems, namely two-dimensional turbulence on a rotating sphere. Although homogeneous isotropic turbulence has been extensively studied in classical fluid mechanics, the fundamental and/or theoretical properties of inhomogeneous anisotropic turbulence are not well known, and the inhomogeneity of two-dimensional turbulence on a rotating sphere is thus not fully understood. Therefore, in this paper, we investigate in detail the mechanism of large-scale zonal flow formation in two-dimensional turbulence on a rotating sphere.

In unforced freely decaying systems, large-scale westward circumpolar zonal flows appear around both poles [1, 2]. In contrast, in forced systems, multiple zonal band structures appear in the first stage of time integration [3, 4]. Then, structures with only two or three very large zonal flows are realized as asymptotic states [4]. Zonal flows in two-dimensional turbulence on a rotating sphere have been extensively studied; however, the mechanism of the zonal flow formation in this system has not been clarified. In the framework of weakly nonlinear analysis, it is known that the existence of viscosity or the decay of incoming waves is necessary for the formation of zonal flows (non-acceleration theorem) [5, 6, 7, 2], but there is no guarantee that this weakly nonlinear theory is available for zonal flow formation in fully nonlinear region. In fact, Obuse and Yamada [13] reported the formation of large-scale westward circumpolar zonal flows in unforced inviscid two-dimensional turbulence on a rotating sphere, which strongly suggests that the underlying factor in the formation mechanism of large-scale zonal flows is not dissipation via viscosity, but the nonlinear terms in the fluid (Euler) equations.

In two-dimensional turbulence on a rotating sphere, wave solutions, called Rossby waves, completely dominate the flow dynamics. The importance of the nonlinear interactions of Rossby waves through the nonlinear terms in the Navier-Stokes or Euler equations is widely recognized. The nonlinear interactions of drift, Rossby, and other linear waves, including the non-local interaction of drift and Rossby waves on the β-plane [8, 9], the near-resonant interaction of internal waves on the β-plane [10], and others [11, 12], have been studied in detail. However, although the β-plane is one of the tangent-plane approximations of a two-dimensional rotating sphere, the nature of the nonlinear terms in the equations of motion in two-dimensional turbulence on a sphere is greatly different from that on a β-plane. Therefore, this paper numerically investigates the three-wave nonlinear interactions of Rossby

waves $Y_n^m \exp(-i\omega t)$, where Y_n^m is the spherical harmonics, that govern the flow dynamics in two-dimensional unforced inviscid turbulence on a rotating sphere in order to clarify the nonlinear interaction involved in the formation of large-scale zonal flows.

This paper first numerically shows that the time-independent part of the governing equation of the flow dynamics alone cannot explain the remarkable growth of the large-scale circumpolar zonal flows around both poles, *i.e.* equatorially symmetrical zonal structures, corresponding to the growth of Rossby waves with an odd total wavenumber n and zero zonal (longitudinal) wavenember m ($i.e. Y_n^0$ with odd n), which is a typical behavior that the flow in this system shows [19]. Then using flow informaiton depending on time, it is shown that three-wave non-local interactions and near-resonant interactions of Rossby waves play important roles for the pronounced growth of Y_n^0 Rossby waves with odd integer n. Furthermore, it is confirmed that the sets of non-local interactions and near-resonant interactions almost perfectly coincide in this system, indicating that non-local near-resonant interaction is the direct factor in the formation of the large-scale westward circumpolar zonal flows.

The remainder of this paper is organized as follows. Section 2 describes the numerical methods used in this study and also briefly introduces the basics of the three-wave nonlinear interaction of Rossby waves. Sections 3 and 4 show the details of the three-wave nonlinear interaction coefficients of Rossby waves and the time derivative of energy of Rossby modes with zonal structures caused by the three-wave non-resonant nonlinear interactions of Rossby waves, respectively. Section 5 discusses the involvement of three-types of interactions, namely non-local, near-resonant, and non-local near-resonant nonlinear interactions, of Rossby waves in the formation of large-scale westward circumpolar zonal flows. Section 6 concludes the paper. Appendices A and B respectively examine the reliability of the values of the nonlinear interaction coefficients calculated in Section 3 and confirm the robustness of the non-local energy transfer in the considered system.

2 Settings

We consider an unforced two-dimensional barotropic incompressible flow on a rotating sphere. The dynamics of such a flow are normally described by the combination of the two-dimensional Navier-Stokes equations and the continu-

ity equation. However, because it is suggested that viscosity is not indispensable for the formation of large-scale westward circumpolar zonal flows [13], for simplicity, we use the following unforced nondimensionalized vorticity equation[1]:

$$\frac{\partial \zeta}{\partial t} + J(\psi, \zeta) + 2\Omega \frac{\partial \psi}{\partial \phi} = 0, \tag{1}$$

which originates not from the Navier-Stokes equations but from the Euler equations. Equation (1) is written with respect to the longitude ϕ and sin(latitude) μ. In the equation, t, $\psi(\phi, \mu, t)$, and $\zeta(\phi, \mu, t) := \nabla^2 \psi$ are the time, stream function, and vorticity, respectively. The rotation rate of the sphere Ω is chosen to be $\Omega = 10^4$ throughout this paper[2]. The nonlinear term is expressed using the Jacobian operator $J(f, g) := (\partial f/\partial \phi)(\partial g/\partial \mu) - (\partial f/\partial \mu)(\partial g/\partial \phi)$.

This system has linear wave solutions called Rossby waves $Y_n^m(\phi, \mu) \exp(-i\omega_n^m t)$, where $Y_n^m(\phi, \mu)$ represents the spherical harmonics ($n \in \mathbb{Z}_+$, $m \in \mathbb{Z}$, $-n \leq m \leq n$). Here, n and m are the total and zonal (longitudinal) wavenumbers, respectively. The linear frequency ω_n^m of the wave is given as

$$\omega_n^m = -\frac{2m\Omega}{n(n+1)}. \tag{2}$$

Hereafter, Rossby waves $Y_n^m \exp(-i\omega_n^m t)$ are sometimes denoted as Y_n^m for brevity and are referred to as "Rossby modes" or simply "modes".

Because spherical harmonics form a complete set in spherical geometry, the dynamics of Rossby waves completely govern the time evolution of two-dimensional turbulence on a rotating sphere. Therefore, when discussing the mechanism of large-scale zonal flow formation based on the concept of Rossby waves, the three-wave nonlinear interactions of Rossby waves through the nonlinear term in Eq. (1) are considered to play an important role.

The necessary conditions for the three-wave nonlinear interaction of Rossby

[1]The length, velocity, and time are respectively nondimensionalized using the radius a of the sphere, the characteristic velocity amplitude $U_0 := \sqrt{2E}$ of the initial state, where E is the mean kinetic energy, and the advection time scale a/U_0.

[2]This value is in the range of Ω where large-scale zonal flow formation can most easily occur.

waves $Y_k^j \times Y_s^r \to Y_n^m$ are [14]

$$m = j + r, \tag{3}$$
$$|k - s| < n < k + s, \tag{4}$$
$$n + k + s = \text{odd integer}. \tag{5}$$

When the additional condition regarding the linear frequencies in Eq. (2)

$$\frac{m}{n(n+1)} = \frac{j}{k(k+1)} + \frac{r}{s(s+1)}, \tag{6}$$

originating from $\omega_n^m = \omega_k^j + \omega_s^r$, is satisfied, the three-wave nonlinear interaction is said to be a three-wave resonant nonlinear interaction [15, 16]. Of note, although the three-wave resonant nonlinear interactions of Rossby waves totally determine the dynamics of the flow field of two-dimensional Rossby wave turbulence, at least within a certain time range when $\Omega \to \infty$ [17, 18], the formation of large-scale zonal flows, which is probably the most characteristic property of this system, cannot be explained by considering only the three-wave resonant nonlinear interactions of Rossby waves. This is because three-wave resonant nonlinear interactions do not transfer any energy to Rossby modes with zonal structures (i.e., Y_n^0; zonal Rossby modes) [16]. This suggests the importance of investigating the three-wave non-resonant nonlinear interactions of Rossby waves. Therefore, in the following sections, we numerically investigate the effect of the three-wave non-resonant nonlinear interactions of Rossby waves on large-scale zonal flow formation.

The flow field data used in Sections 3, 4, and 5 are obtained by the temporal integration of Eq. (1) using the spectral method, where, for example, the stream function and the vorticity are expanded as

$$\psi(\phi, \mu, t) = \sum_{n=0}^{N_T} \sum_{m=-n}^{n} \psi_n^m(t) Y_n^m(\phi, \mu), \tag{7}$$
$$\zeta(\phi, \mu, t) = \sum_{n=0}^{N_T} \sum_{m=-n}^{n} \zeta_n^m(t) Y_n^m(\phi, \mu) \tag{8}$$
$$= \sum_{n=0}^{N_T} \sum_{m=-n}^{n} -n(n+1)\psi_n^m(t) Y_n^m(\phi, \mu). \tag{9}$$

We take 512 and 256 spatial grid points in the longitudinal and latitudinal directions, respectively, and set the truncation wavenumber $N_T = 170$ to

eliminate aliasing errors[3]. The obtained ordinary differential equations are integrated using the fourth-order Runge-Kutta method with a time step of $dt = 4.0 \times 10^{-5}$. The initial condition is set using the energy spectrum

$$E_n(t) = \begin{cases} \displaystyle\sum_{m=-n}^{n} E_n^m(t) = \sum_{m=-n}^{n} \frac{1}{2} n(n+1)(\psi_n^m(t))^2 = \frac{A n^{\gamma/2}}{(n+n_0)^\gamma}, \quad n_0 = 50, \quad \gamma = 100, \ (n \geq 2) \\ 0, \ (n = 0, 1) \end{cases} \tag{10}$$

where A is defined such that

$$\sum_{n=2}^{N_T} E_n(t) = 1.0, \tag{11}$$

at $t = 0$. The values of E_n^m for fixed n that satisfy the conditions in Eqs. (10) and (11) are set at random[4]. The peak of the initial energy distribution is set rather low here because this study focuses on the formation of large-scale zonal flows, which is a phenomenon that occurs in low-wavenumber region.

The energy spectra E_n and E_n^m and the longitudinal component of velocity at initial time $t = 0$ and 10 are shown in Fig. 1. A zonal structure, specifically large-scale westward circumpolar zonal flows around both poles, appears and develops over time. This is the result of the energy accumulation to zonal Rossby modes Y_n^0. The structure becomes clearly visible around $t \sim 0.8$ in the calculation (data not shown). After a sufficiently long time ($t = 10$ for example), there is strong energy accumulation to zonal Rossby modes with a low total wavenumber ($n \lesssim 15$), which correspond to the flow field with large-scale westward circumpolar zonal flows. Significant energy accumulation occurs in low-wavenumber regions where the total wavenumber n is an odd integer; far less energy accumulates in those where n is an even integer. This trend, which has been previously reported [19], also appears in the time variation of the system. Figure 2 shows the clear difference observed in the behavior of the total energy of zonal Rossby modes with odd- and even-integer n in our numerical calculation. This difference is a key point in our discussion of the mechanism of large-scale zonal flow formation throughout this paper.

[3]The spatial resolution of this numerical calculation is rather coarse. However, we confirmed that further increasing the resolution does not significantly affect the time evolution of the resulting flow field [13].

[4]Most of the results shown in this paper were confirmed to have the same tendency for different random distributions of the initial E_n^m.

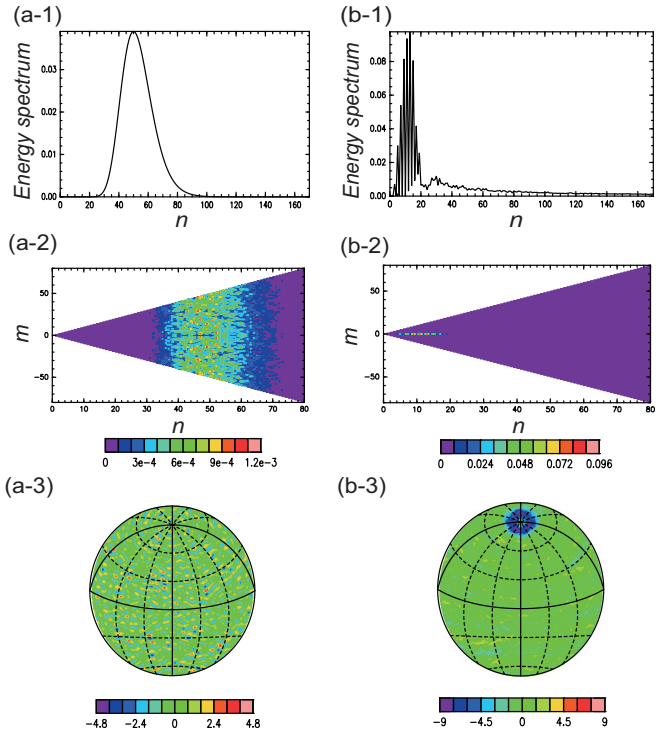

Figure 1: Energy spectrum E_n at (a-1) $t = 0$ and (b-1) $t = 0.8$. Energy spectrum E_n^m at (a-2) $t = 0$ and (b-2) $t = 0.8$. Only the wavenumber region $0 \leq n \leq 80$, $-n \leq m \leq n$ is shown for visibility, as little energy is distributed in high-wavenumber region. Longitudinal component of velocity at (a-3) $t = 0$ and (b-3) $t = 10$. Negative values correspond to westward flow and positive values to eastward flow. The sphere is tilted 20 degrees in the direction of latitude to make it easier to see the flow field around the North Pole.

3 Three-wave nonlinear interaction coefficients

In this section, we calculate the three-wave nonlinear interaction coefficients to determine whether the difference in the behavior of zonal Rossby modes

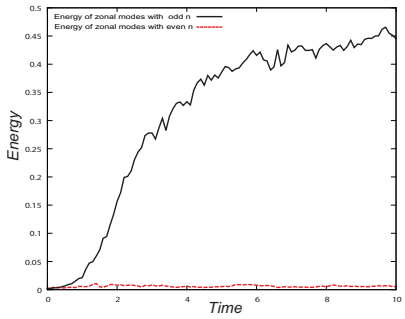

Figure 2: Time variation of total energy of zonal Rossby modes with odd-integer n (black solid curve) and even-integer n (red dashed curve) from $t = 0$ to 10.

with respect to the parity of n originates from the *time-independent part* of the nonlinear term of the vorticity equation in Eq. (1). According to Silberman [14], the time evolution of the spectral components of the stream function can be expressed as

$$\frac{d\psi_n^m(t)}{dt} = \frac{2i\Omega m\psi_n^m(t)}{n(n+1)} + \frac{i}{2}\sum_{s=0}^{N_T}\sum_{r=-s}^{s}\sum_{k=0}^{N}\sum_{j=-k}^{k}\psi_k^j(t)\psi_s^r(t)H_{kns}^{jmr}, \tag{12}$$

which is equivalent to the equation of motion in Eq. (1). Here, H_{kns}^{jmr} represents the coefficients of the three-wave nonlinear interactions via the nonlinear term in Eq. (1). Note that unlike the case in the β-plane model, Eq. (1) involves a large number of nonlinear couplings among spherical harmonics. The first term on the right-hand side is derived from the linear term. The second term on the right-hand side is derived from the nonlinear term, which is the sum of the effect on ψ_n^m from all the possible three-wave nonlinear interactions among ψ_k^j, ψ_s^r, and ψ_n^m.

In this study, since we particularly want to know the time evolution of the Rossby modes that correspond to the zonal flows, hereafter we consider the case $m = 0$, which makes the first term on the right-hand side zero. Therefore, the significant difference in the time evolution of ψ_n^m that depends on the parity of n arises only from the second term on the right-hand side of Eq. (12).

For the case $m = 0$, according to Silberman [14], H_{kns}^{jmr} is expressed as

$$H_{kns}^{j0-j} = \frac{s(s+1) - k(k+1)}{n(n+1)} L_{kns}^{j0-j}, \tag{13}$$

$$\begin{aligned} L_{kns}^{j0-j} &= (-1)^j L_{nks}^{0jj} \\ &= (-1)^j \{E_{nks}^{0jj} - E_{skn}^{jj0}\} \\ &= (-1)^j E_{nks}^{0jj}, \end{aligned} \tag{14}$$

$$E_{nks}^{0jj} = j\sqrt{2n+1} \sum_q \sqrt{2q+1} \int_0^\pi P_q^0 P_k^j P_s^j \sin\theta d\theta, \tag{15}$$

if the conditions in Eqs. (3), (4), and (5) and the condition

$$j, m, r \geq 0 \tag{16}$$

are satisfied. Here, $q = k-1, k-3, k-5, \cdots, j+1$ or j and P_a^b in Eq. (15) is the associated Legendre function [20]. Furthermore, it is known that $P_{ace}^{bdf} := \int_0^\pi P_a^b P_c^d P_e^f \sin\theta d\theta$ can be written as

$$\begin{aligned} P_{ace}^{bdf} = & \frac{(e+a-c-1)!![(2c+1)(2a+1)(2e+1)]^{\frac{1}{2}}}{(e+c-a)!!(a+c-e)!!(c+a+e+1)!!} \\ & \times \left[\frac{(c+d)!(c-d)!(a-b)!(e-f)!}{2(a+b)!(e+f)!}\right]^{\frac{1}{2}} \\ & \times \sum_{h=0}^{c-d} \frac{(-1)^{\frac{1}{2}(e-a+c)+f+h}(e+f+h)!(a+c-f-h)!}{(c-d-h)!h!(e-f-h)!(a-c+f+h)!}, \end{aligned} \tag{17}$$

where $x!! = x(x-2)(x-4)\cdots 2$ or 1, and $0!! = (-1)!! = 1$ [21]. Here, for the definition of P_{ace}^{bdf}, it is necessary to impose

$$a + c + e = \text{even integer}, \tag{18}$$

$$|e-a| < c < e+a. \tag{19}$$

Here, we calculate H_{kns}^{j0-j}, which is the coefficient of the three-wave nonlinear interaction contributing to $d\psi_n^0/dt$, for all the combinations of $(n,0), (k,j), (s,-j)$ for $N_T = 170$, that is

$$0 \leq n, k, s \leq 170,\ -k \leq j \leq k,\ -s \leq -j \leq s, \tag{20}$$

using Eqs. (13), (14), (15), and (17). The reliability of the obtained data is confirmed in Appendix A.

Figure 3 shows the frequency distribution of H_{kns}^{j0-j}, excluding the cases $H_{kns}^{j0-j} = 0$, for n = 1-60 [5]. There is a strong peak and a symmetry around $H_{kns}^{j0-j} = 0$ for all the considered n. Since H_{kns}^{j0-j} takes a non-zero value even when n is an even integer (Figs. 3 and 4), it is not guaranteed that the value of $d\psi_n^0/dt$ always vanishes when n is a low even integer. Little energy increase in Rossby modes with an even-integer n in the time variation of the flow field described in Section 2 may be, at least partially, the result of the cancellation of a huge number of weak interactions in the summations in Eq. (12). In Fig. 3, the parity of n does not cause a significant difference and so it may be that the strong development of modes with a low odd-integer n is not caused simply by the nonlinear interaction coefficients (i.e., the time-independent part of the nonlinear term), but is caused by the combination of the nonlinear interaction coefficients and the state of the flow field. This suggests that there is a specific flow field that facilitates large-scale zonal flow formation, which also means that particular set of three-wave nonlinear interaction of Rossby waves play a dominant role in large-scale zonal flow formation.

4 Energy transfer to zonal Rossby modes

Here, we examine the time derivative of the energy of zonal Rossby modes dE_n^0/dt at certain times in the course of time development to confirm its consistency with the development of large-scale zonal flow formation, and also to obtain a starting point for the investigation of three-wave nonlinear interactions. The time evolution of the energy spectrum of zonal modes is expressed as

$$\frac{dE_n^0}{dt} = n(n+1)\frac{d\psi_n^0}{dt}\psi_n^0. \tag{21}$$

We calculated this using the values of H_{kns}^{j0-j} obtained in Section 3 and the flow field data (i.e., numerical data of the stream function) shown in Section 2.

[5] As the focus here is on the formation of large-scale zonal flows, we are only interested in the energy transfer to Y_n^0 modes with a low n.

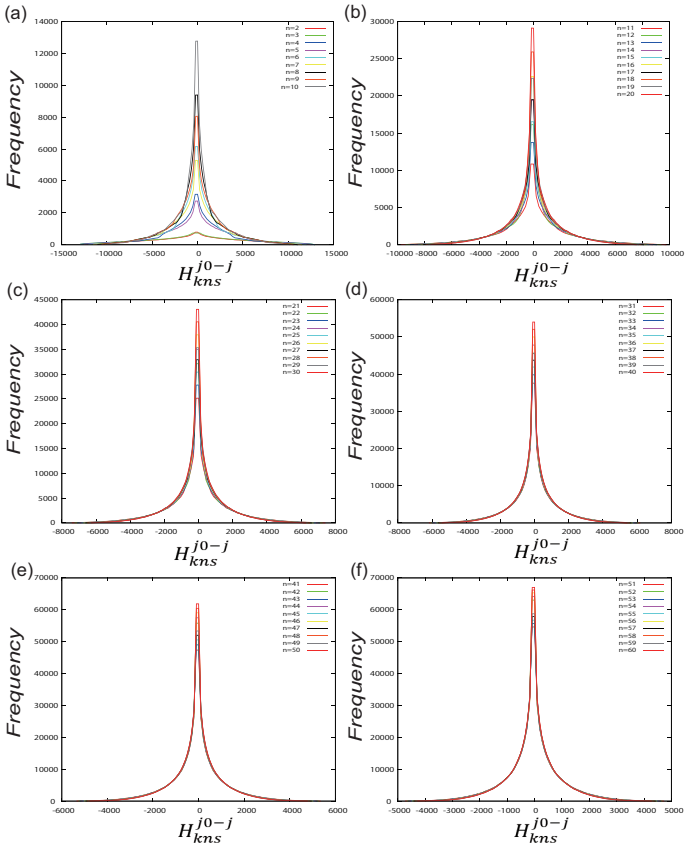

Figure 3: Frequency distribution of H_{kns}^{j0-j}, excluding cases $H_{kns}^{j0-j} = 0$, for (a) n = 2-10, (b) n = 11-20, (c) n = 21-30, (d) n = 31-40, (e) n = 41-50, and (f) n = 51-60.

Figure 5 shows dE_n^0/dt at various times. As shown, there is a non-zero energy transfer to modes with a low ($n \lesssim 15$) odd-integer n even at $t = 0.1$ (i.e., the very beginning of time integration). The large-scale zonal flows are

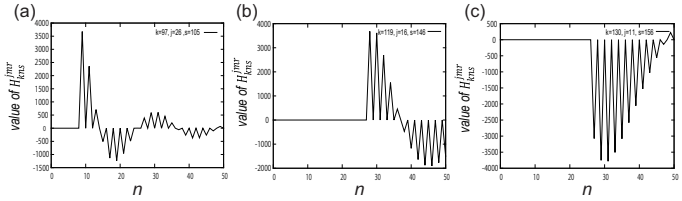

Figure 4: Examples of H^{j0-j}_{kns} for n = 1-50. (a) $(k, j, s, -j) = (119, 16, 146, -16)$, (b) $(k, j, s, -j) = (97, 26, 105, -26)$, and (c) $(k, j, s, -j) = (130, 11, 156, -11)$.

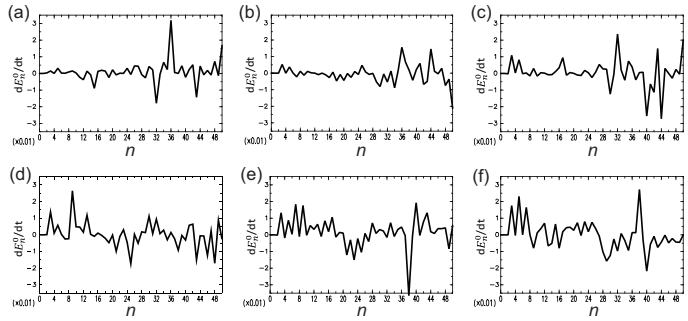

Figure 5: Time derivative of the energy of zonal Rossby modes dE^0_n/dt for n = 0-50 at (a) $t = 0.1$, (b) $t = 0.15$, (c) $t = 0.2$, (d) $t = 0.5$, (e) $t = 0.8$, and (f) $t = 1.0$.

not visible at this time (data not shown), which means that low-wavenumber modes do not have much energy yet. This suggests the existence of non-local energy transfer; we will come back to this point in Section 5. It is also confirmed that the amount of energy transfer to such modes gradually increases until $t = 0.7$, when zonal flows become visible.

Figure 6 shows an overplot of dE^0_n/dt from $t = 0$ to $t = 3.0$ increments of 0.01. Figures 5 and 6 suggest that the energy transfer to zonal modes with a low odd-integer n almost always takes a positive value. Energy thus accumulates in such zonal modes. On the other hand, zonal modes with a

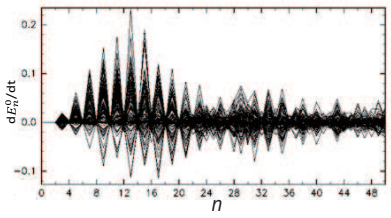

Figure 6: Overplot of the time derivative of the energy of zonal Rossby modes dE_n^0/dt from $t = 0$ to $t = 3.0$ in increments of 0.01.

low even-integer n take almost zero values at each instant, probably as a result of the cancellation of the effects from many interactions in the summation in Eq. (12). However, the dE_n^0/dt with low even-integer n is not necessarily exactly zero and the small non-zero dE_n^0/dt values almost cancel out again when integrated over time. The modes with a mid to high n tend to take non-zero dE_n^0/dt values. The probabilities of taking positive and negative values seem to be quite the same regardless of the parity of n. Then dE_n^0/dt may almost cancel out over time, yielding very small E_n^0 values in mid to high n region after a sufficiently long time. This is consistent with the strong development of zonal modes with a low odd-integer n, corresponding to the circumpolar flows described in Section 2. However, this information is insufficient to explain the mechanism of large-scale zonal flow formation. Therefore, in the following section, the time derivative of the energy of zonal Rossby modes dE_n^0/dt is investigated in more detail.

5 Large-scale zonal flow formation via nonlocal interactions and near-resonant interactions

In this section, we numerically investigate the three-wave non-resonant nonlinear interactions of Rossby waves that directly transfer energy to large-scale westward circumpolar zonal flows by focusing on the time derivative of the energy of zonal Rossby modes dE_n^0/dt with a low n.

5.1 Non-local interactions

In Section 4, it was suggested that the energy is transferred to the zonal modes with a low wavenumber even at the very beginning of time integration, when most energy is distributed in the mid- to high-wavenumber regions. Therefore, in this section, we first see the development of the time variation of the energy spectrum E_n^m.

Figure 7 shows the energy spectrum E_n^m at $t = 0.08$ to $t = 0.8$ (i.e., early to middle stages of large-scale zonal flow formation). It can be seen that at $t = 0.3$, high values suddenly appear at $m = 0$ and $n = 3, 5, 7$, which are close to the lowest possible odd integer ($n = 3$). However, most energy is still distributed in the mid- to high-wavenumber regions at this time and modes with a low wavenumber other than Y_3^0, Y_5^0, or Y_7^0 still do not have much energy. The high energy values suddenly appear, as if they had jumped over the $8 \lesssim n \lesssim 16$ region. This suggests that the large-scale westward circumpolar zonal flows are formed by the energy non-locally transferred to low-n zonal Rossby modes. This point is verified below.

For the three-wave nonlinear interaction $Y_k^j \times Y_s^r \to Y_n^m$, the definitions of the three-wave *non-local* and *local* interactions used in this paper are as follows[6]:

$$\text{non-local: } \min(k, s) - n \geq \frac{a}{100} \min(k, s), \tag{22}$$

$$\text{local: } \min(k, s) - n < \frac{a}{100} \min(k, s), \tag{23}$$

where a is set to 40. The definition in Eq. (22) is a weaker condition than the criterion used by Rose and Sulem [22].

By using the definitions in Eqs. (22) and (23), we calculate dE_n^0/dt due to the three-wave non-local and local nonlinear interactions

$$\left(\frac{dE_n^0}{dt}\right)_{\text{non-local}} = \frac{i}{2} \sum_{\substack{\text{non-local} \\ \text{interactions}}} \psi_k^j \psi_s^{-j} H_{kns}^{j0-j}, \tag{24}$$

and

$$\left(\frac{dE_n^0}{dt}\right)_{\text{local}} = \frac{i}{2} \sum_{\substack{\text{local} \\ \text{interactions}}} \psi_k^j \psi_s^{-j} H_{kns}^{j0-j}. \tag{25}$$

[6]Because of the inverse cascade of energy, we suppose that $\min(k, s) > n$.

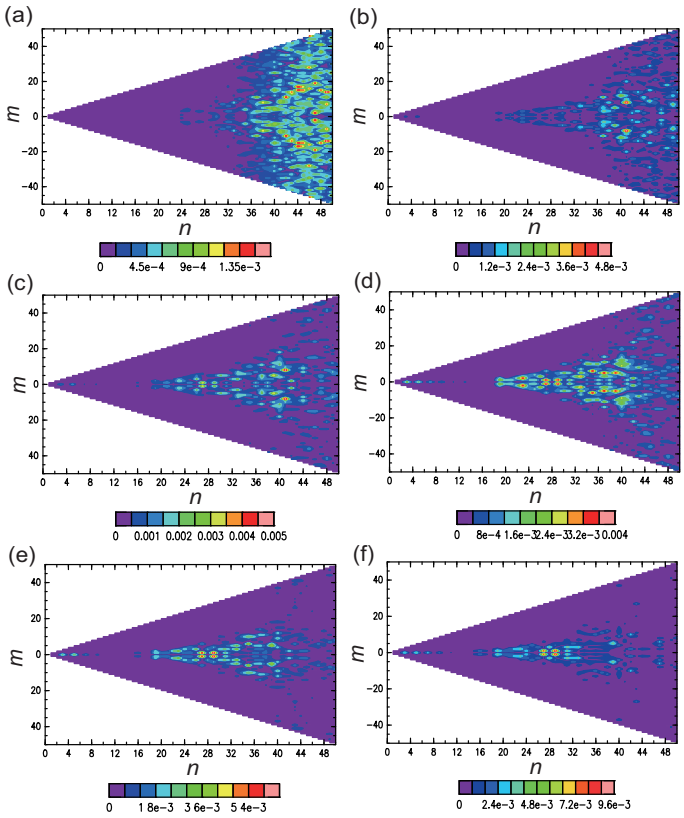

Figure 7: Energy spectrum E_n^m at (a) $t = 0.1$, (b) $t = 0.3$, (c) $t = 0.5$, (d) $t = 0.6$, (e) $t = 0.7$, and (f) $t = 0.8$. Only the wavenumber region $0 \leq n \leq 50$, $-n \leq m \leq n$ is shown for visibility. Little energy is distributed in high-wavenumber region.

As done in Section 4, the values of H_{kns}^{j0-j} obtained in Section 3 and the flow field data (i.e., numerical data of the stream function) shown in Section 2 are used.

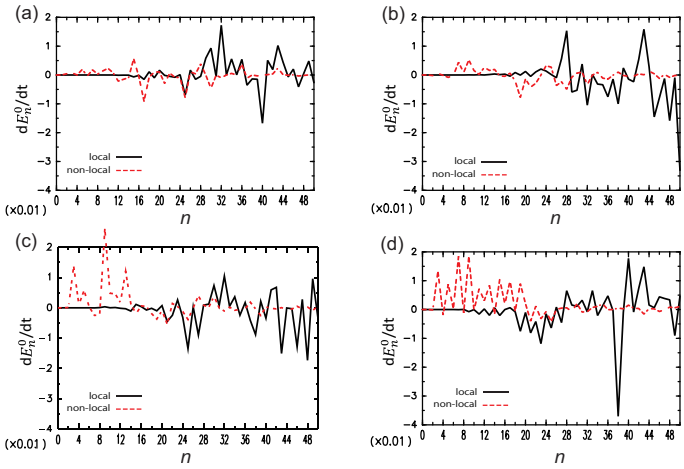

Figure 8: Time derivative of energy of zonal Rossby modes dE_n^0/dt caused by non-local and local nonlinear interactions at (a) $t = 0.08$, (b) $t = 0.3$, (c) $t = 0.5$, and (d) $t = 0.8$. Red dashed lines indicate non-local interaction and black solid lines indicate local interaction.

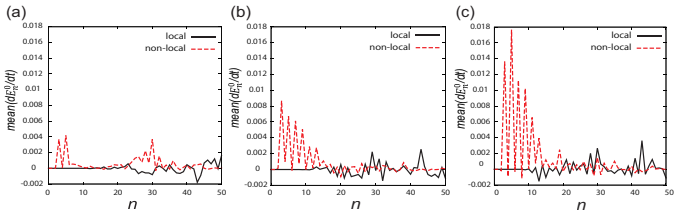

Figure 9: Time-mean of dE_n^0/dt caused by non-local and local nonlinear interactions at (a) t = 0.0-0.3 (initial stage of large-scale zonal flow formation), (b) t = 0.3-0.6 (middle stage of large-scale zonal flow formation), and (c) t = 0.6-0.9 (late stage of large-scale zonal flow formation). Red dashed lines indicate non-local interaction and black solid lines indicate local interaction.

Figure 8 shows dE_n^0/dt caused by non-local and local interactions at var-

ious times and Fig. 9 shows the time-mean of dE_n^0/dt for three time periods. Non-local energy transfer to zonal modes with a low odd-integer n already occurs at $t = 0.08$ and tends to increase with time, whereas local energy transfer to low-n modes is always almost zero. This tendency is more clearly shown by the time-mean of dE_n^0/dt (Fig. 9), suggesting the importance of non-local energy transfer in the large-scale zonal flow formation in this system (further confirmation of the robustness of non-local energy transfer in this system is given in Appendix B).

5.2 Near-resonant interactions

We next consider the fact that the growth of zonal Rossby modes Y_n^0 differs significantly depending on the parity of the total wavenumber n; specifically, zonal modes with an odd-integer n show large growth and become dominant, whereas modes with an even-integer n show little growth, as shown in Fig. 2 [19]. When considering the factors that give rise to the difference in the characteristics of zonal Rossby modes depending on the parity of n in terms of nonlinear interactions, one important point is the relation to three-wave resonant nonlinear interactions. Among zonal Rossby modes, all modes with an odd-integer n satisfy the three-wave resonant nonlinear interaction condition in Eq. (6) as one of the elements of at least one resonant triad (resonant zonal modes), whereas no modes with an even-integer n can be an element of any resonant triad (non-resonant zonal modes) [16, 19]. With this and given the importance of the three-wave resonant interactions of Rossby waves in two-dimensional rotating systems [17, 18], here we investigate the development of zonal Rossby modes from the perspective of three-wave resonant nonlinear interactions. It is worth noting that three-wave resonant interactions do not directly transfer energy to zonal modes, as stated in Section 2 [16]. We thus investigate near-resonant interactions, which are non-resonant interactions but may have properties similar to those of resonant interactions.

Whereas three-wave resonant interaction has a clear definition given in Eq. (6), there is, to the best of the authors' knowledge, no established definition for three-wave near-resonant interaction. Therefore, in this study, for the three-wave nonlinear interaction $Y_k^j \times Y_s^r \to Y_n^m$, we define the *near-resonant* interaction condition as

$$0 < \left| \frac{m}{n(n+1)} - \left(\frac{j}{k(k+1)} + \frac{r}{s(s+1)} \right) \right| \leq \epsilon \mathrm{Ro}, \tag{26}$$

based on the definition of near-resonant interaction for internal waves given by Smith and Lee [10]. Here, ϵ is set to 1.1, $\mathrm{Ro} := U/(2\Omega L)$ is the Rossby number (Fig. 10(a)), where the length scale of the flow field L is defined as the energy-weighted wavelength $L := \sum_n (nE_n)/\sum_n E_n$ (Fig. 10(b)), and the scale of the flow field velocity U is defined as $U := \sqrt{2E}$ using the spatial mean of the kinematic energy E of the flow[7, 8]. Non-resonant interactions that do not satisfy the near-resonant interaction condition in Eq. (26) are genuine non-resonant interactions and are referred to as *far-resonant* interactions in this paper. The definition of far-resonant interaction is therefore

$$\left| \frac{m}{n(n+1)} - \left(\frac{j}{k(k+1)} + \frac{r}{s(s+1)} \right) \right| > \epsilon \mathrm{Ro}. \tag{27}$$

By using the definitions in Eqs. (26) and (27), we calculate dE_n^0/dt due to the near-resonant and far-resonant nonlinear interactions

$$\left(\frac{dE_n^0}{dt} \right)_{\text{near-resonant}} = \frac{i}{2} \sum_{\substack{\text{near-resonant} \\ \text{interactions}}} \psi_k^j \psi_s^{-j} H_{kns}^{j0-j}, \tag{28}$$

and

$$\left(\frac{dE_n^0}{dt} \right)_{\text{far-resonant}} = \frac{i}{2} \sum_{\substack{\text{far-resonant} \\ \text{interactions}}} \psi_k^j \psi_s^{-j} H_{kns}^{j0-j}. \tag{29}$$

As done in Section 4 and Section 5.1, the values of H_{kns}^{j0-j} obtained in Section 3 and the flow field data (i.e., numerical data of the stream function) shown in Section 2 are used.

Figure 11 shows dE_n^0/dt caused by near-resonant and far-resonant interactions at various times. It can be seen that energy transfer via near-resonant

[7] For the definition of U, $U := |\min(\mathrm{mean}_{lon}(u_\phi(\phi, \mu, t)))|$, where u_ϕ is the longitudinal component of fluid velocity, may also be reasonable, especially when large-scale circumpolar zonal flows have already formed. However, as we are mainly interested in the formation process of large-scale circumpolar zonal flows, we use $U = \sqrt{2E}$ in this paper.

[8] We also considered the following definition of three-wave near-resonant nonlinear interaction:

$$0 < \left| \frac{m}{n(n+1)} - \left(\frac{j}{k(k+1)} + \frac{r}{s(s+1)} \right) \right| \leq \frac{a}{100} \max \left(\frac{j}{k(k+1)}, \frac{r}{s(s+1)} \right),$$

based on an idea similar to that used for the definitions of non-local and local interactions given in Eqs. (22) and (23). We obtained similar results with $a \gtrsim 35$.

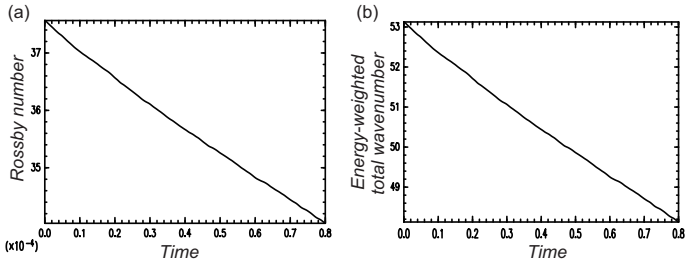

Figure 10: Time variation of (a) Rossby number Ro and (b) energy-weighted wavelength from $t = 0.0$-0.8.

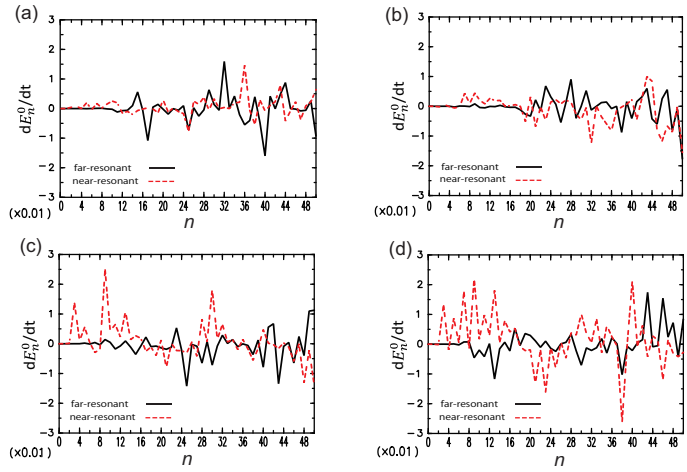

Figure 11: Time derivative of energy of zonal Rossby modes dE_n^0/dt caused by near-resonant and far-resonant nonlinear interactions at (a) $t = 0.08$, (b) $t = 0.3$, (c) $t = 0.5$, and (d) $t = 0.8$. Red dashed lines indicate near-resonant interaction and black solid lines indicate far-resonant interaction.

interactions to zonal modes with a low odd-integer n is always dominant. This tendency is more clearly seen in the time-mean of $dE_{n_c}^0/dt$ shown in

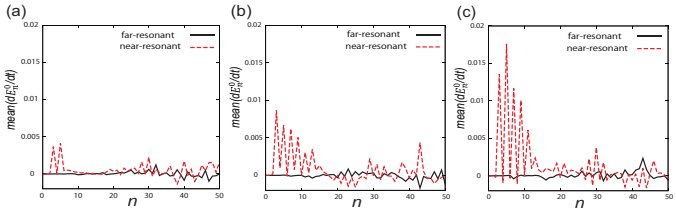

Figure 12: Time-mean of dE_n^0/dt caused by near-resonant and far-resonant interactions at (a) t = 0.0-0.3 (initial stage of large-scale zonal flow formation), (b) t = 0.3-0.6 (middle stage of large-scale zonal flow formation), and (c) t = 0.6-0.9 (late stage of large-scale zonal flow formation). Red dashed lines indicate near-resonant interaction and black solid lines indicate far-resonant interaction.

Fig. 12. This suggests that only near-resonant interactions are directly involved in the energy transfer to zonal Rossby modes with a low odd-integer n (i.e., the formation of large-scale circumpolar zonal flows), while both near-resonant and far-resonant interactions contribute to the energy transfer to zonal modes with a mid or high total wavenumber n.

5.3 Non-local near-resonant interactions

As described in Section 5.1 and Section 5.2, both non-local interactions and near-resonant interactions are directly involved in the formation of large-scale circumpolar zonal flows. However, non-local interaction and near-resonant interaction are completely different concepts and thus the sets of non-local interactions and near-resonant interactions may not coincide.

Figures 13–16 show the time derivative of energy of zonal Rossby modes dE_n^0/dt caused by four types of nonlinear interaction, namely NN : {non-local}$\cap$ {near-resonant}, NF : {non-local}$\cap${far-resonant}, LN : {local}$\cap${near-resonant}, and LF : {local}$\cap${far-resonant} interactions. It is observed that large positive dE_n^0/dt values appear for zonal Rossby modes with a low odd-integer total wavenumber ($n \lesssim 15$), which correspond to the large-scale westward circumpolar zonal flows, caused by non-local near-resonant (NN) nonlinear interactions (Fig. 13), while only small positive or negative dE_n^0/dt and almost zero dE_n^0/dt caused by non-local far-resonant (NF) interactions (Fig. 14)

and local (local near-resonant (LN) and local far-resonant (LF)) interactions (Figs. 15 and 16), respectively, are seen for $n \lesssim 15$. Zonal Rossby modes with a higher total wavenumber ($n \gtrsim 15$) have positive or negative dE_n^0/dt values regardless of the type of nonlinear interaction, which suggests that any type of interaction can function in the $n \gtrsim 15$ region.

The importance of non-local near-resonant (NN) interactions for the formation of large-scale westward circumpolar zonal flows is more clearly demonstrated in the time-mean plot of dE_n^0/dt. In this plot, large positive values are observed for $n \lesssim 15$ due to NN interactions (Fig. 17), while the time-mean values of dE_n^0/dt for $n \lesssim 15$ are almost zero for other types of interaction (Figs. 18–20).

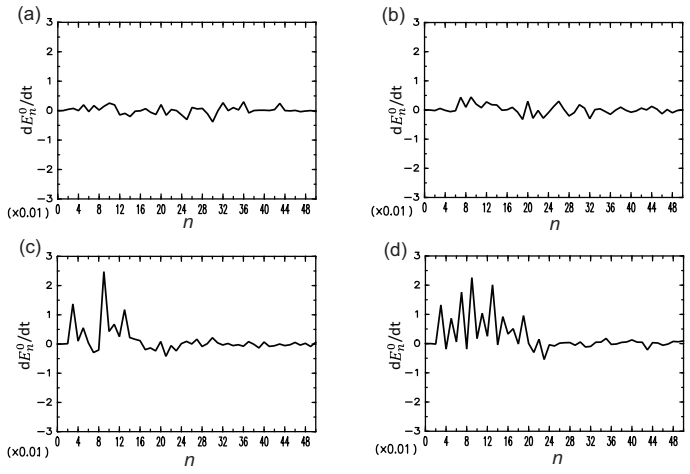

Figure 13: Time derivative of energy of zonal Rossby modes dE_n^0/dt caused by NN interactions at (a) $t = 0.08$, (b) $t = 0.3$, (c) $t = 0.5$, and (d) $t = 0.8$.

The numbers of total nonlinear, non-local, local, resonant, near-resonant, and far-resonant interactions at $t = 0.5$ are shown in Table I. The time variation of the numbers of non-local, near-resonant, and non-local near-resonant (NN) interactions are shown in Fig. 21. About 95% of non-local interactions are non-local near-resonant (NN) interactions and about 5% are non-local far-resonant (NF) interactions. From this and the observation of

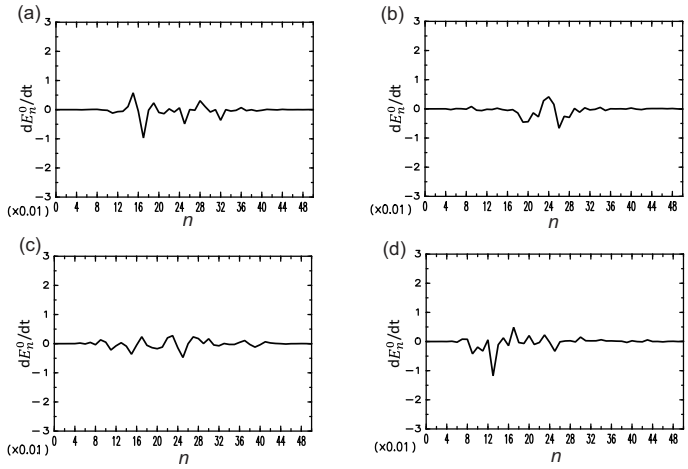

Figure 14: Time derivative of energy of zonal Rossby modes dE_n^0/dt caused by NF interactions at (a) $t = 0.08$, (b) $t = 0.3$, (c) $t = 0.5$, and (d) $t = 0.8$.

dE_n^0/dt caused by four types of interaction shown above, it appears that the set of non-local interactions and the set of near-resonant interactions in this system are almost perfectly coincident, and that Non-local near-resonant (NN) interactions are a direct factor in the formation of large-scale westward circumpolar zonal flows. The existence of non-local far-resonant (NF) interactions may have resulted from the incompleteness of the definition of near-resonant interaction used here. Even if NF interaction is intrinsic to this system, NF interactions are unlikely to directly affect the formation of large-scale westward circumpolar zonal flows.

6 Conclusions

In unforced two-dimensional turbulence on a rotating sphere, large-scale westward zonal flows are formed around both poles [1, 2], but the mechanism is not yet fully understood. As the formation of large-scale zonal flows occurs without the effect of viscous dissipation [13], the nonlinear interaction

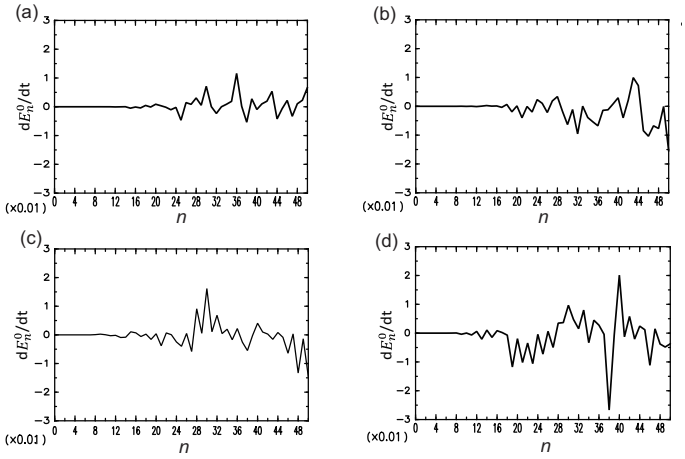

Figure 15: Time derivative of energy of zonal Rossby modes dE_n^0/dt caused by LN interactions at (a) $t = 0.08$, (b) $t = 0.3$, (c) $t = 0.5$, and (d) $t = 0.8$.

Table I: Numbers of interactions at $t = 0.5$. Only the numbers of rear-resonant and far-resonant interactions depend on time.

Interaction type	Including cases $H_{kns}^{j0-j} = 0$	Excluding cases $H_{kns}^{j0-j} = 0$
Nonlinear	7449250	7358625
Non-local	6342821	6282135
Local	1106429	1076490
Resonant	90625	0
Near-resonant	6491943	6491943
Far-resonant	866682	866682

of Rossby waves via the nonlinear terms in the equations of motion is considered to be a fundamental factor. Therefore, in this paper, given that the three-wave resonance interaction of Rossby waves does not transfer energy to zonal Rossby modes [16] and considering that among zonal Rossby modes Y_n^0 only modes with an odd-integer n acquire energy and grow [19], the three-wave non-resonant nonlinear interactions of Rossby waves were investigated

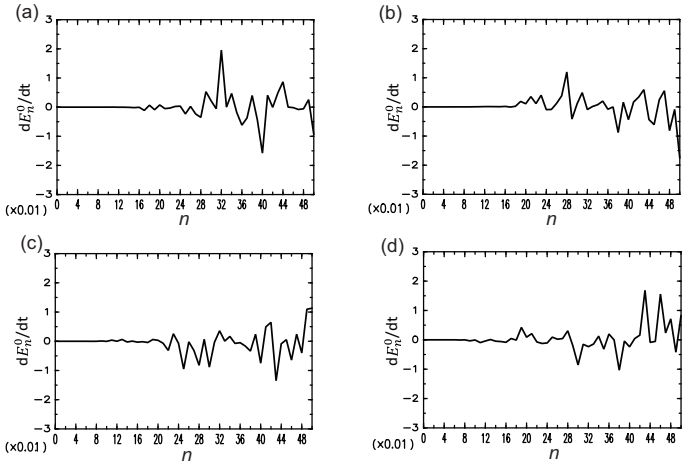

Figure 16: Time derivative of energy of zonal Rossby modes dE_n^0/dt caused by LF interactions at (a) $t = 0.08$, (b) $t = 0.3$, (c) $t = 0.5$, and (d) $t = 0.8$.

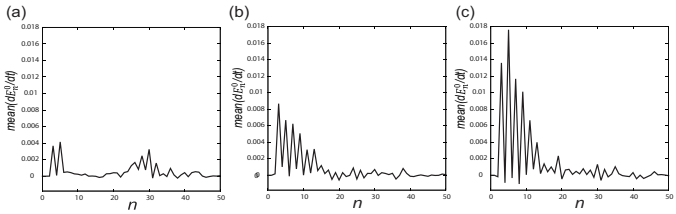

Figure 17: Time-mean of dE_n^0/dt caused by NN interactions at (a) $t = 0.0$–0.3 (initial stage of large-scale zonal flow formation), (b) $t = 0.3$–0.6 (middle stage of large-scale zonal flow formation), and (c) $t = 0.6$–0.9 (late stage of large-scale zonal flow formation).

in detail.

In Section 3, the coefficients of each three-wave nonlinear interaction H_{kns}^{j0-j} were calculated. It was found that this time-independent information alone cannot explain the difference in the growth rate of zonal Rossby

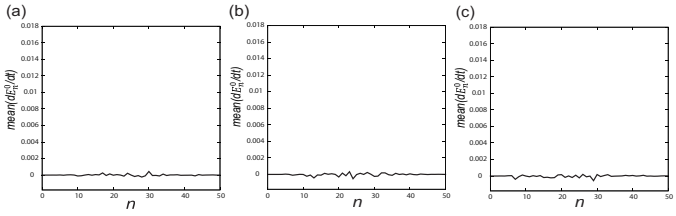

Figure 18: Time-mean of dE_n^0/dt caused by NF interactions at (a) $t = 0.0$–0.3 (initial stage of large-scale zonal flow formation), (b) $t = 0.3$–0.6 (middle stage of large-scale zonal flow formation), and (c) $t = 0.6$–0.9 (late stage of large-scale zonal flow formation).

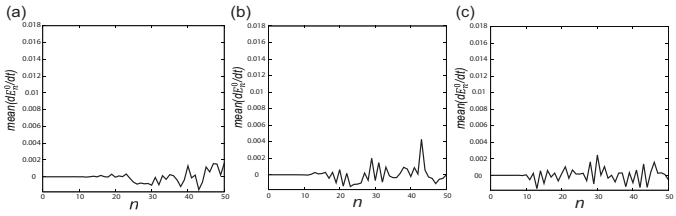

Figure 19: Time-mean of dE_n^0/dt caused by LN interactions at (a) $t = 0.0$–0.3 (initial stage of large-scale zonal flow formation), (b) $t = 0.3$–0.6 (middle stage of large-scale zonal flow formation), and (c) $t = 0.6$–0.9 (late stage of large-scale zonal flow formation).

modes depending on the parity of n even at a given time instant, in other words, we also need to take into account the state of the flow field to understand the formation of large-scale zonal flows. Then in Section 4, the time derivative of the energy of each zonal Rossby mode dE_n^0/dt, which is the combination of the nonlinear interaction coefficients H_{kns}^{j0-j} and the flow field data, was calculated. It was found that dE_n^0/dt almost always takes positive value when n is a low odd integer and is zero or a very small non-zero value when n is a low even integer. This suggests the existence of two types of cancellation that lead to little energy growth of zonal Rossby modes (Y_n^0) with a low even-integer n. Most of the non-zero contributions from the many three-wave nonlinear interactions involved at each time instant cancel

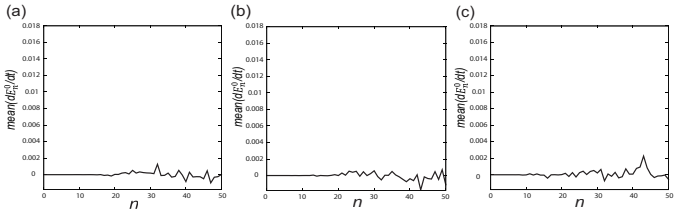

Figure 20: Time-mean of dE_n^0/dt caused by LF interactions at (a) $t = 0.0$–0.3 (initial stage of large-scale zonal flow formation), (b) $t = 0.3$–0.6 (middle stage of large-scale zonal flow formation), and (c) $t = 0.6$–0.9 (late stage of large-scale zonal flow formation).

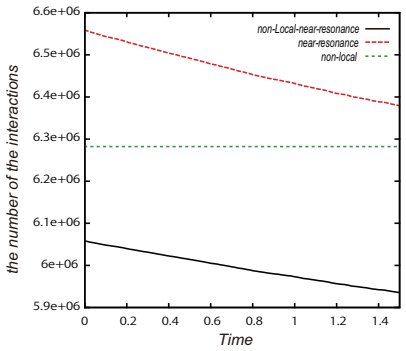

Figure 21: Numbers of non-local, near-resonant, and non-local near-resonant (NN) interactions from $t = 0.0$ to 1.5.

with each other to give a small dE_n^0/dt. Furthermore, this small dE_n^0/dt at each time instant is almost cancelled again as a result of time integration; the mechanism of such cancellations is not clear. To further investigate the three-wave nonlinear interactions that directly affect the development of only zonal Rossby modes with a low odd-integer n, among the three-wave non-resonant nonlinear interactions, we focused on non-local interactions, near-resonant interactions, and non-local near-resonant interactions, and investigated their effects on the time derivative of the energy of zonal Rossby modes dE_n^0/dt in

Sections 5.1, 5.2, and 5.3. The results confirmed that the formation of the large-scale westward circumpolar zonal flows is directly caused by non-local energy transfer due to near-resonant interactions.

It is often said that the locally interacting energy cascade is important in turbulence. However, this paper showed that it is the non-local interactions that are most important in the considered system. This may be strongly related to the compactness of the considered flow field domain. When we consider the two-dimensional flow on a sphere, as in this paper, the flow domain is compact and the basic modes are discrete. Therefore, the nonlinear interactions must be non-local, especially in the low-wavenumber region. For the two-dimensional turbulence on a β-plane, the importance of the non-local interactinos of waves is discussed, for example, in Balk *et al.* [9], while a picture of the local energy transfer was proposed by Takaoka *et al.* [23] under a locality assumption of the energy transfer. This is the nonlocality observed even when the wavenumbers are continuous. In the case of spherical geometry, however, the wavenumbers themselves are naturally discrete, which is the point characteristic of spherical case and different from β-plane. The importance of near-resonant interactions is intuitively understandable because resonant interactions are the strongest interactions in this system, but do not affect zonal Rossby modes. In numerical calculations, not only does it happen that the non-local near-resonant interaction defined in this paper works strongly due to the geometric constraint mentioned above, but the flow field evolves in time from a random homogeneous initial state so that the non-local near-resonant interaction dominates. During the time evolution process from a random homogeneous initial state to a flow field where non-local near-resonant interactions become dominant, interactions other than non-local near-resonant interactions may coordinate the flow field. The formation of large-scale zonal flows in two-dimensional turbulence on a rotating sphere is directly caused by non-local near-resonant interactions, but is also achieved indirectly through the complex combinations of other three-wave non-resonant interactions and also resonant interactions [19][9]. The role of each type of nonlinear interaction should be investigated in detail to get a better understanding of their mutual influence. This may contribute not only to the clarification of the mechanism of large-scale zonal flow formation in two-dimensional turbulence on a rotating sphere but also to the realization

[9]Although three-wave resonant interactions do not transfer any energy to zonal modes, they influence the time variation of non-resonant modes and should thus not be ignored.

of the control of large-scale zonal flow formation in systems with a similar mathematical structure.

Acknowledgements

Kiori Obuse was supported by the Japan Society for the Promotion of Science (JSPS) through KAKENHI grants 21K03352, 17H02860, and 21H05309. Michio Yamada was supported by the JSPS through KAKENHI grants 21K03352 and 17H02860. This work was partially supported by the Research Institute for Mathematical Sciences, and International Joint Usage/Research Center located at Kyoto University. This work was also partially supported by the "Initiative for Realizing Diversity in the Research Environment" from MEXT. The authors would like to thank the Isaac Newton Institute for Mathematical Sciences, Cambridge, for support and hospitality during the programme "Layering — A structure formation mechanism in oceans, atmospheres, active fluids and plasmas", which was supported by EPSRC grant no EP/R014604/1, where work on this paper was undertaken. Some of the data analysis and visualizations in this paper were performed with the ISPACK library (http://www.gfd-dennou.org/library/ispack/), the gt4f90io library (http://www.gfd-dennou.org/libgary/gtool/), SPMODEL [24] (http://www.gfd-dennou.org/library/spmodel/), and software developed by the GFD Dennou Ruby project (http://ruby.gfd-dennou.org/). The numerical calculations were performed using the supercomputer JSS3 of the Japan Aerospace Exploration Agency (JAXA) and the computer systems of the Research Institute for Mathematical Sciences, Kyoto University.

Appendix A: Reliability of obtained three-wave nonlinear interaction coefficients H_{kns}^{j0-j}

The numerical calculation of the equations in Silberman's notation given in Eqs. (13)–(19) to obtain the coefficients of three-wave nonlinear interactions H_{kns}^{j0-j} in Section 3 may introduce significant errors (e.g., the loss of trailing digits and the cancellation of significant digits). Therefore, the obtained data were cross-checked as follows. We consider a flow field consisting of only $Y_k^{\pm j}$ and $Y_s^{\pm j}$ Rossby waves, where the time derivative of the component of the stream function ψ_n^0 caused by nonlinear interactions of $Y_k^{\pm j}$ and $Y_s^{\mp j}$ is

expressed as

$$\frac{d\psi_n^0}{dt} = \frac{[J(\psi_k^j Y_k^j, \zeta_s^{-j} Y_s^{-j}) + J(\psi_k^{-j} Y_k^{-j}, \zeta_s^j Y_s^j)]_n^0}{n(n+1)}. \tag{30}$$

Note that for non-zero nonlinear interaction, the condition in Eq. (3) should be satisfied, which means that nonlinear interactions between Rossby waves with the same superscript (e.g., $Y_k^j \times Y_s^j$) do not occur. The time derivative of the component of the stream function ψ_n^0 caused by nonlinear interactions of $Y_k^{\pm j}$ and $Y_s^{\mp j}$ can also be written as

$$\frac{d\psi_n^0}{dt} = \frac{i}{2}\left(\psi_k^j \psi_s^{-j} H_{kns}^{j0-j} + \psi_k^{-j} \psi_s^j H_{kns}^{-j0j}\right), \tag{31}$$

using the nonlinear interaction coefficients. We calculate Eq. (30) using the spectral method, as described in Section 2, and Eq. (31) using Silberman's notation given in Eqs. (13)–(19) and the data of the stream function described in Section 2. The examples of relative errors for different combinations of k, s, and j are shown in Fig. 22. The absolute value of relative errors is quite small, less than 1.0×10^{-5}, confirming that the values of the obtained nonlinear interaction coefficients are reliable.

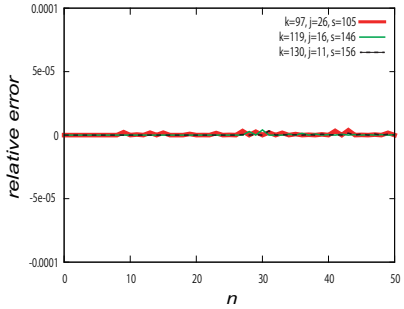

Figure 22: Relative error of $d\psi_n^0/dt$ between Eqs. (30) and (31). Red thick solid line: $(k, j, s, -j) = (97, 26, 105, -26)$, thin green solid line: $(k, j, s, -j) = (119, 16, 146, -16)$, black dashed line: $(k, j, s, -j) = (130, 11, 156, -11)$.

Appendix B: Robustness of non-local energy transfer

As a confirmation of the robustness of the non-local energy transfer in this system, we conducted a numerical experiment that restricts the passage of energy through modes with n = 20-40 and checked whether the energy can be transferred to the lower-n ($n < 20$) modes from higher-n ($n > 40$) modes via non-local interactions of Rossby waves.

The initial energy distribution was similar to the standard initial energy distribution in this paper, given in Eqs. (10) and (11), but the energy in n = 20-40 modes was discarded, as shown in Figs. 23(a-1) and (a-2). The flow field corresponding to this energy distribution is shown in Fig. 23(a-3). We let the flow field vary according to the vorticity equation in Eq. (1), but restricted the passage of energy through modes with n = 20-40 by discarding all the energy of such modes at each time step of the numerical time integration.

The energy spectrum and longitudinal component of velocity at $t = 0.8$ and $t = 2.5$ are shown in Figs. 23(b) and (c). It can be seen that even when modes with n = 20-40 are not involved in the time variation of the flow field, energy is non-locally transferred to the low-n modes to form large-scale zonal flows. The temporal variation of the spatial-mean kinetic energy is shown in Fig. 24. There is almost no energy decrease from $t = 0$ to $t = 2.5$[10], which suggests that the existence of n = 20-40 modes were not indispensable for the inverse energy cascade that formed large-scale circumpolar zonal flows in this numerical experiment. This is consistent with the importance of the non-local nonlinear interactions of Rossby waves in the formation of large-scale circumpolar zonal flows, as shown in Fig. 9.

References

[1] S. Yoden and M. Yamada, "A numerical experiment on two-dimensional decaying turbulence on a rotating sphere", *J. Atomos. Sci.* **50**, 631–643 (1993)

[2] S. Takehiro, M. Yamada, and Y.-Y. Hayashi, "Energy accumulation in easterly circumpolar jets generated by two-dimensional barotropic

[10] The amount of energy decrease is only about 0.5%.

decaying turbulence on a rapidly rotating sphere", *J. Atmos. Sci.* **64**, 4084–4097 (2006)

[3] T. Nozawa and S. Yoden, "Formation of zonal band structure in forced two-dimensional turbulence on a rotating sphere", *Phys. Fluids* **9**, 2081–2093 (1997)

[4] K. Obuse, S. Takehiro, and M. Yamada, "Long-time asymptotic states of forced two-dimensional barotropic incompressible flows on a rotating sphere", *Phys. Fluids.* **22**, 156601 (2010)

[5] G. Charney and P.G. Drazin, "Propagation of planetary-scale disturbances from the lower into the upper atmosphere", *J. Geophys. Res.* **6**6, 83–110 (1961)

[6] A. Eliassen and E. Palm, "On the transfer of energy in stationary mountain waves", *Geofys Publ.*, **22(3)**, 1–23 (1961)

[7] D.G. Andrews and M.E. McIntyre, "Planetary waves in horizontal and vertical shear: The generalized Eliassen-Palm relation and the mean zonal acceleration", *J. Atoms. Sci.*, **30(11)**, 2031–2048 (1976)

[8] A.M. Balk and S.V. Nazarenko, "On the nonlocal turbulence of drift type waves", *Phys. Lett. A*, **146(4)**, 217–221 (1990)

[9] A.M. Balk, V.E. Zakharov, and S.V. Nazarenko, "Nonlocal turbulence of drift waves", *Sov. Phys. JETP*, **71(2)**, 249–260 (1990)

[10] L. Smith and Y. Lee, "On near resonances and symmetry breaking in forced rotating flows at moderate Rossby number", *J. Fluid Mech*, **535**, 111–142 (2005)

[11] E. Kartashova, Nonlinear Resonance Analysis (Cambridge University Press, 2010).

[12] V.E. Zakharov, V.S. L'vov, and G. Falkovich, Kolmogorov Spectra of Turbulence I: Wave Turbulence (Springer, 1992).

[13] K. Obuse and M. Yamada, Manuscript in preparation.

[14] I. Silberman, "Planetary waves in the atmosphere", *J. Meteor.* **11**, 27–34 (1953)

[15] G.M. Reznik, L.I. Piterbarg, and E.A. Kartashova, "Nonlinear interactions of spherical Rossby modes", *Dyn. Atoms. Oceans* **18**, 235–252 (1993)

[16] K. Obuse and M. Yamada, "Three-wave resonant interactions and zonal flows in two-dimensional Rossby–Haurwitz wave turbulence on a rotating sphere", *Phys. Rev. Fluids* **4**, 024601 (2019)

[17] M. Yamada and T. Yoneda, "Resonant interaction of Rossby waves in two-dimensional flow on a β plane", *Physica D* **245(17)**, 1–7 (2013)

[18] A. Dutrifoy and M. Yamada, Manuscript in preparation.

[19] K. Obuse and M. Yamada, "Energy transfer to resonant zonal Rossby modes in two-dimensional turbulence on a rotating sphere", *J. Phys. Soc. Jpn.*, **89**, 064401 (2020)

[20] M. Abramowitz and I.A. Stegun (eds), Handbook of Mathematical Functions: with Formulas, Graphs, and Mathematical Tables (Dover Books on Mathematics, 1964)

[21] L. Infeld and T.E. Hull, "The Factorization Method", *Rev. Mod. Phys.*, **23**, 21 (1951)

[22] H.A. Rose and P.L. Sulem, "Fully developed turbulence and statistical mechanics", *Journal de Physique*, **39(5)**, 441–484 (1978)

[23] M. Takaoka, N. Yokoyama, and E. Sasaki, "Local-flux vectores of conserved quantities in wavenumber space: Anisotropic structures in Charney-Hasegawa-Mima turbulence", *Phys. Rev. Fluids*, **7**. L012601 (2022)

[24] S. Takehiro, M. Odaka, K. Ishioka, M. Ishiwatari, Y.-Y. Hayashi, and SPMODEL Development Group, "A series of hierarchical spectral models for geophysical fluid dynamics", *Nagare Multimedia* (2006) Available on-line at: http://www.nagare.or.jp/mm/2006/spmodel/

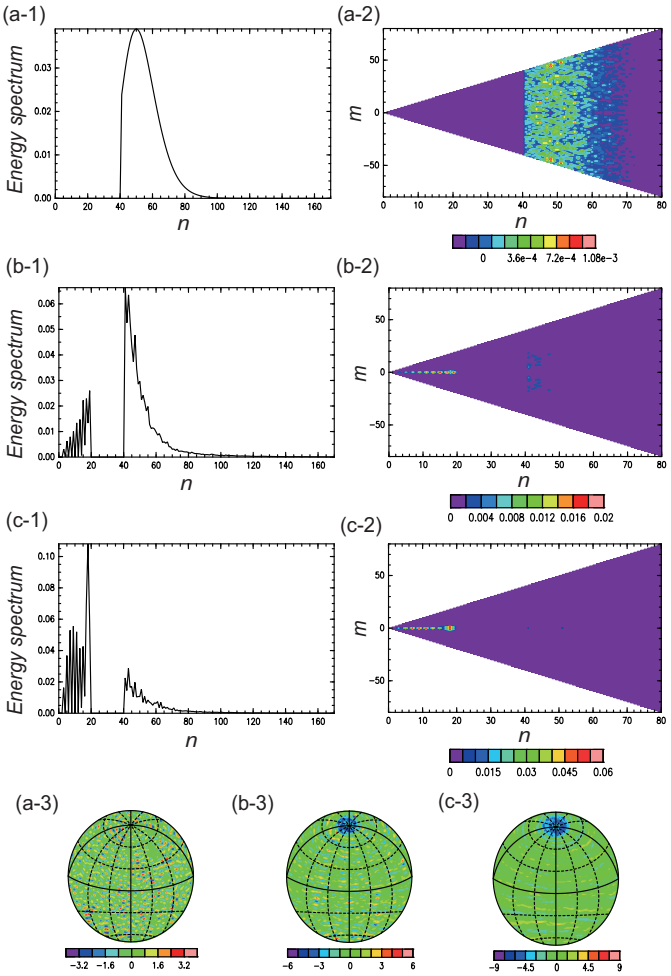

Figure 23: Energy spectrum E_n at (a-1) $t = 0$, (b-1) $t = 0.8$, and (c-1) $t = 2.5$. Energy spectrum E_n^m at (a-2) $t = 0$, (b-2) $t = 0.8$, and (c-2) $t = 2.5$ (only the wavenumber region $0 \leq n \leq 80$, $-n \leq m \leq n$ is shown for visibility; little energy is distributed in high-wavenumber regions). Longitudinal component of velocity at (a-3) $t = 0$, (b-3) $t = 0.8$, and (c-3) $t = 2.5$ when passage of energy through modes with $n = 20$–40 is restricted by discarding all the energy of such modes at each time step of the numerical time integration. Negative values correspond to westward flow and positive values to eastward flow. The sphere is tilted 20 degrees in the direction of latitude to make it easier to see the flow field around the North Pole.

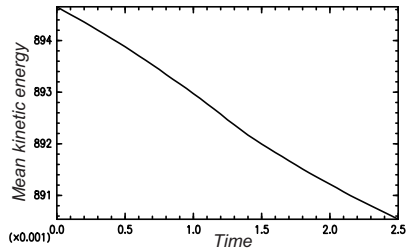

Figure 24: Time variation of spatial-mean kinetic energy from $t = 0$ to $t = 2.5$ when passage of energy through modes with $n = 20$-40 is restricted by discarding all the energy of such modes at each time step of the numerical time integration.